

ORIGINAL ARTICLE

Green and eco-friendly biosynthesis of zinc oxide nanoparticles using *Calendula officinalis* flower extract: Wound healing potential and antioxidant activity

Cigdem Aydin Acar^{1,2}  | Muhammet Abdurrahim Gencer²  |
Suray Pehlivanoglu³  | Sukriye Yesilot^{1,2}  | Soner Donmez⁴ 

¹Department of Nursing, Bucak School of Health, Burdur Mehmet Akif Ersoy University, Burdur, Turkey

²Department of Health and Biomedical Sciences, Burdur Mehmet Akif Ersoy University, Burdur, Turkey

³Department of Molecular Biology and Genetics, Faculty of Science, Necmettin Erbakan University, Konya, Turkey

⁴Bucak School of Health, Burdur Mehmet Akif Ersoy University, Burdur, Turkey

Correspondence

Cigdem Aydin Acar, Department of Nursing, Bucak School of Health, Burdur Mehmet Akif Ersoy University, Burdur, Turkey.

Email: cacar@mehmetakif.edu.tr

Funding information

Burdur Mehmet Akif Ersoy University Scientific Research Projects Unit, Grant/Award Number: 0792-YL-21

Abstract

This study aimed to produce zinc oxide nanoparticles with *Calendula officinalis* flower extract (Co-ZnO NPs) using the green synthesis method. In addition, the antioxidant and wound healing potential of synthesized ZnO NPs were evaluated. The absorbance band at 355 nm, which is typical for ZnO NPs, was determined from the UV-Vis absorbance spectrum. The energy-dispersive X-ray spectroscopy (EDS) measurements revealed a high zinc content of 42.90%. The x-ray diffractometer data showed Co-ZnO NPs with an average crystallite size of 17.66 nm. The Co-ZnO NPs did not have apparent cytotoxicity up to 10 µg/mL (IC₅₀ 25.96 µg/mL). *C. officinalis* ZnO NPs showed partial cell migration and percent wound closure (69.1%) compared with control (64.8%). In addition, antioxidant activities of Co-ZnO NPs with 2,2'-azino-bis(3-ethylbenzothiazoline-6-sulfonic acid) (ABTS) and 2,2 diphenyl-1 picrylhydrazil (DPPH) were evaluated and radical scavenging activity of 33.49% and 46.63%, respectively, was determined. These results suggest that *C. officinalis* extract is an effective reducing agent for the green synthesis of ZnO NPs with significant antioxidant and wound healing potential.

KEYWORDS

antioxidant, *Calendula officinalis*, green synthesis, wound healing, zinc oxide nanoparticles

Key Messages

- In this study, zinc oxide nanoparticle synthesis and characterization were carried out for the first time using the *Calendula officinalis* plant with a green and environmentally friendly biosynthesis method.
- The cytotoxicity of the synthesized zinc oxide nanoparticles in L929 cells was evaluated and the wound healing effect was evaluated in L929 cells in vitro with the determined therapeutic dose.
- The antioxidant activity was also evaluated.
- The study is an original study in terms of evaluating the wound healing effects of zinc oxide nanoparticles.

This is an open access article under the terms of the [Creative Commons Attribution-NonCommercial](https://creativecommons.org/licenses/by-nc/4.0/) License, which permits use, distribution and reproduction in any medium, provided the original work is properly cited and is not used for commercial purposes.

© 2023 The Authors. *International Wound Journal* published by Medicalhelplines.com Inc and John Wiley & Sons Ltd.

1 | INTRODUCTION

Diabetes mellitus is a metabolic disease characterised by high blood sugar. According to the data of the World Health Organization (WHO), there are approximately 422 million diabetic patients worldwide and 1.5 million people die from diabetes every year. Both the number of cases and the prevalence of diabetes have been increasing steadily over the past few decades.¹ Drugs currently available for the treatment are of various classes such as sulfonylureas, thiazolidinedione, α -glucosidase inhibitors, repaglinide and insulin treatments. Unfortunately, the most widely used drug metformin has various side effects and shows a slow therapeutic response.² Therefore, there is a need to develop new therapeutic drugs. According to the WHO, about 80% of the world's population consider traditional medicines to be the best for the treatment of various diseases. Medicinal plants are considered extremely beneficial in many ways in combating various diseases, including diabetes.^{1,3–5} At the same time, most complications of diabetes are due to oxidative stress accompanied by a decrease in the cellular content of zinc and zinc-dependent antioxidant enzymes. Zinc has roles in homeostasis, immune function, defence against oxidative stress and apoptotic cell death. In addition, it effectively cures type 2 diabetes and its complications.^{6,7} In the last few years, many nanomaterials have been designed and researched for the healing of chronic wounds, one of the complications of diabetes. Especially metal-based nanomaterials are of great interest. These include metal oxide nanoparticles (NPs) such as silver, gold, iron, copper, titanium and zinc oxide (ZnO) NPs. These NPs have proven effective in eradicating multidrug-resistant strains and promoting wound healing and re-epithelialisation.^{8,9}

Nanotechnology is an important and developing science for the development of an environmentally friendly and reliable methodology, which aims to develop materials with dimensions of 1–100 nm, which has become increasingly important in recent years.¹⁰ NPs find wide use in the health, food, aerospace, pharmaceutical and cosmetic industries. Nanotechnology deals with the molecular scale properties of nanostructures such as size, shape, surface morphology and applications, and the interface between the chemical, biological, physical, optical and electronic properties of nanomaterials.¹¹ With the development of industrial production at nanoscale, metal oxides such as silver oxide (AgO), gold oxide (AuO), titanium dioxide (TiO₂), copper oxide (CuO) and cerium oxide (CeO₂) have found a wide market area.¹² Thanks to medical and pharmaceutical applications, NPs of noble

metals such as gold, silver, platinum and ZnO are widely applied.¹³

Three different synthesis methods have been developed for NPs: physical, chemical and green syntheses. Expensive equipment, high temperature and high pressure are required in NP synthesis by physical methods. In the synthesis of NPs by chemical methods, toxic chemicals that can cause serious damage to the environment and living things are used.¹⁴ Due to the disadvantages of physical and chemical synthesis, these methods have been replaced by green synthesis, which is an eco-friendly and cost-effective method. Biological resources containing various natural molecules such as plants, bacteria, fungi and algae are used for the green synthesis of NPs.^{15–18} NPs produced from plant extracts are more stable and more diverse in shape and size than those produced by other organisms.¹⁹ Among metal oxide NPs, ZnO NPs have been at the forefront of research due to their unique properties and wide range of applications.²⁰

In particular, the use of the extracts of medicinal plants as potential reducing and stabilizing agents to synthesize ZnO NPs provides many advantages over traditional, physical and highly toxic chemical methods.²¹ The advantages of ZnO NPs over other metal NPs are due to their lower cost, UV blocking properties, high catalytic activity, large surface area, as well as their remarkable applications in medicine, environmental remediation, antimicrobial activity and agriculture.^{22–24} Various plant extracts have been successfully used for efficient and rapid extracellular biosynthesis of ZnO NPs, for example, *Pongamia pinnata*,²⁵ *Vitex trifolia*,²⁶ *Ficus benghalensis*,²⁷ *Punica granatum*,²⁸ *Trifolium pratense*,²⁹ *Hibiscus subdariffa*³⁰ and *Couroupita guianensis* Aubl.³¹

Calendula officinalis is an annual plant of Mediterranean origin. It is known that its medicinal use is mostly from the 13th century and especially in the direction of wound healing. It was used as balms and creams during the North American Civil War and as antiseptic and anti-inflammatory agents during World War I.³² It has medicinal uses as an anti-inflammatory agent, particularly for the treatment of wounds, first-degree burns, contusions and skin eruptions. German health authorities recommended superficial use in leg ulcers and internal use against inflammatory lesions in the oral and pharyngeal mucosa. The main chemical components found in its flowers are saponins, triterpenes, alcohol triterpenes, fatty acid esters, carotenoids, flavonoids, coumarins, essential oils, hydrocarbons and fatty acids.^{33,34} In this study, it was aimed for the first time to synthesise ZnO NPs with calendula (*C. officinalis*) flower plant extract and to evaluate the wound healing, antioxidant and cytotoxic activities of these NPs.

2 | MATERIALS AND METHODS

2.1 | Preparation of aqueous extract of *C. officinalis* flower

The dried flowers of *C. officinalis* were purchased from a local market (Arifoğlu Spice and Food Ind. Trade. Ltd. Sti) and used for extraction. 10 g of dried calendula flowers was weighed and transferred to a 500-mL container. 100 mL of distilled water was added to it. This mixture was heated at 100°C for 2 h on a magnetic stirrer. After this process, the mixture brought was to room temperature and passed through Whatman No.1 filter paper. The filtrate was stored in a refrigerator at +4°C until used for NP synthesis.

2.2 | Green synthesis of ZnO NPs

Zinc nitrate hexahydrate ($\text{Zn}(\text{NO}_3)_2 \cdot 6\text{H}_2\text{O}$) as the zinc precursor was purchased from Sigma–Aldrich. 50 mL of filtered *C. officinalis* flower aqueous extract was boiled at 60–80°C using a magnetic stirrer and 5 g of zinc nitrate hexahydrate was added. The mixture was heated continuously on a magnetic stirrer until it reduced to 10 mL or turned into a paste. The resulting ZnO NPs were dried in an oven at 60°C overnight. The obtained Co-ZnO NPs was stored in the tube at room temperature until further use.³⁵

2.3 | Characterization of green-synthesised ZnO NPs

The optical properties of ZnO NPs were characterized by taking ultraviolet–visible (UV–Vis) region spectra between 300 and 700 nm. UV–Vis spectral analysis was performed on T60 UV–visible spectrophotometer (PG Instruments). The surface morphology and elemental composition of Co-ZnO NPs were observed using scanning electron microscope (SEM) (FEI Quanta FEG 250) with energy-dispersive X-ray spectroscopy (EDS). Co-ZnO NPs' structure and composition were analysed using x-ray diffractometer (XRD) (Bruker D8 Advance Twin-Twin). SEM, EDS and XRD analyses were carried out at Suleyman Demirel University YETEM—Innovative Applications and Research Center.

2.4 | Cell culture

L929 mouse fibroblast cells belonging to the American Type Culture Collection (ATCC, Manassas, VA) were

used in this study. L929 cells were cultured in Dulbecco's Modified Eagle's Medium (DMEM) (Sigma D6429) containing 10% fetal bovine serum (FBS) (Pan Biotech P30-3303) and 1% antibiotic/antimycotic solution (100×) (Capricorn Scientific AAS-B). The cells were grown in T-75 flasks in a 5% CO_2 atmosphere at 37°C until they reached confluence. The cultured cells were removed with the help of 0.25% Trypsin (Biowest L0909) and passaged. The morphological changes of the cells were checked under an inverted microscope (Olympus CK40).

2.5 | MTT assay

MTT (3-[4,5-Dimethylthiazole-2-yl]-2,5-diphenyltetrazolium bromide) measurement is the colorimetric detection of viable cells at a certain cell density. Cells were seeded on 96-well cell culture plates and incubated with different concentrations of Co-ZnO NPs (0, 1, 5, 10, 20, 30, 40, 50, 100, 200 $\mu\text{g}/\text{mL}$) for 48 h in an incubator with 5% CO_2 at 37°C.³⁶ After incubation, cytotoxicity testing was performed using the MTT cell proliferation measurement kit (Sigma M5655). After the incubation with different concentrations of Co-ZnO NPs was completed, the medium was discarded and 100 μL of fresh medium was added. 10 μL of MTT stock solution (5 mg/mL of stock in phosphate buffered saline (PBS)) was added to the cells and incubated for 4 h in the dark at 37°C with 5% CO_2 . The mixture in each well was aspirated, and 100 μL of dimethyl sulfoxide (DMSO) was added to dissolve the purple formazan. After incubation, the optical density (OD) of the plate was measured at a 570 nm wavelength using a microplate reader (MultiscanGO, Thermo Fisher Scientific, USA). The MTT assay was repeated three times. Results were expressed as the mean percentage of cell growth. The percentage (%) of cell viability was calculated using the following formula:

$$\text{Cell viability (\%)} = \text{OD treatment} / \text{OD control} \times 100.$$

The concentration value (IC_{50}) that reduced the viability of L929 cells to 50% was determined based on the dose-dependent cell viability curve.

2.6 | In vitro wound healing assay

The wound healing assay used to measure the migration rate of a population of cells on scratched surfaces was used to evaluate the migratory ability of L929 cells after exposure to Co-ZnO NPs. To determine the wound

healing ability, exponentially growing fibroblast cells were seeded in a 6-well culture plate at a density of 5×10^5 cells/well and incubated for 24 h.³⁷ The culture medium was changed periodically. After confluence was achieved in the cells, a linear area in the cell monolayer was scraped using a sterile 100- μ L plastic pipette tip, and the cells were washed with PBS to remove cell debris. Cells were then treated with a fresh medium containing 10 μ g/mL Co-ZnO NPs and cultured for 16 and 24 h. The control group was prepared with a basal medium. The plotted areas were photographed from each cell culture well using an inverted microscope (Olympus CK40) to assess the distance between adjacent cell layers. Wound areas were measured using Image-J analysis software. The percentage of wound closure was calculated according to the following formula:

$$\text{Wound closure (\%)} = \frac{(A_0 - A_t)}{A_0} * 100$$

where A_0 is the scratch wound area recorded at hour 0 and A_t is the scratch wound area recorded at time X.

2.7 | ABTS radical scavenging activity

2,2'-azino-bis(3-ethylbenzothiazoline-6-sulfonic acid) (ABTS) radical scavenging activity was performed according to the method described by Re et al.³⁸ 7 mM ABTS and 2.45 mM potassium persulfate ($K_2S_2O_8$) were combined in equal volumes and incubated for 16 h in the dark and at room temperature. Co-ZnO NPs were prepared with methanol at different concentrations (0–1000 μ g/mL). In the control sample, methanol was used instead of plant extract. In the test mixture, 100 μ L of sample and 2.9 mL of ABTS solution were mixed and incubated in the dark for 30 min. Ascorbic acid was used as a positive control. The absorbance of samples was measured at 734 nm wavelength using a spectrophotometer (T60 UV-PG Instruments). The % inhibition is calculated using the following formula:

$$\% \text{inhibition} = \frac{(A_{\text{control}} - A_{\text{sample}})}{A_{\text{control}}} * 100$$

where A_{control} is the absorbance of negative control and A_{sample} is the absorbance of sample.

2.8 | DPPH radical scavenging activity

Antioxidant activity of Co-ZnO NPs was determined using 2,2-diphenyl-1-picrylhydrazil (DPPH). The method

was modified³⁹ and ascorbic acid was used as the standard. 1000 μ L of DPPH solution in methanol (0.1 mM) was added to the samples containing 1000 μ L of Co-ZnO NP. After adding DPPH to the samples, they were incubated for 30 min at room temperature and in the dark, and their absorbance was measured at 517 nm (T60 UV-PG Instruments). As a negative control, methanol was used instead of the sample. The % inhibition is calculated using the following formula:

$$\% \text{inhibition} = \frac{(A_{\text{control}} - A_{\text{sample}})}{A_{\text{control}}} * 100$$

where A_{control} is the absorbance of negative control and A_{sample} is the absorbance of sample.

2.9 | Statistical analysis

The statistical analysis of data was expressed as mean \pm SEM. The Student's *t*-test was used for statistical comparison and differences were considered significant at $p \leq 0.05$. All experiments were performed at least three times. GraphPad Prism 9 program was used to calculate IC_{50} and SD.

3 | RESULTS AND DISCUSSION

3.1 | Synthesis and characterization of ZnO NPs

Addition of zinc nitrate hexahydrate to *C. officinalis* extract caused physico-chemical changes in aqueous solution. The most obvious one of these changes is in colour that can be observed in the reaction mixture. In this study, the colour change from yellow to brown and a pale yellow colour solid precipitate in *C. officinalis* extract, respectively, indicated the formation of Co-ZnO NPs (Figure 1). Within a few hours, the colour of the solution stopped changing, suggesting that the ZnO salt was completely bioreduced to ZnO NPs. Flavonoids and phenolic compounds are responsible for the conversion of Zn ions to ZnO NPs. Phytochemicals are antioxidants and non-toxic chemicals; therefore, they can act as both reducing and stabilizing agents.⁴⁰ These results were consistent with studies reporting colour changes in plant-mediated green synthesis of ZnO NPs.^{41,42} There is no report on the use of *C. officinalis* plant extract in the green synthesis of ZnO NPs. However, its use in the synthesis of silver and selenium NPs has been reported.^{43,44}

Figure 2 shows the UV-Vis absorption spectrum of green-synthesised ZnO NPs. An absorbance peak around

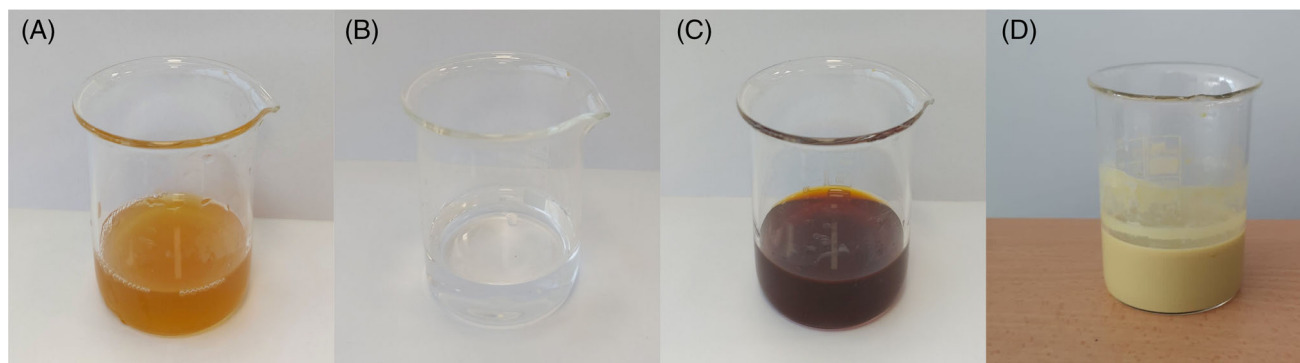
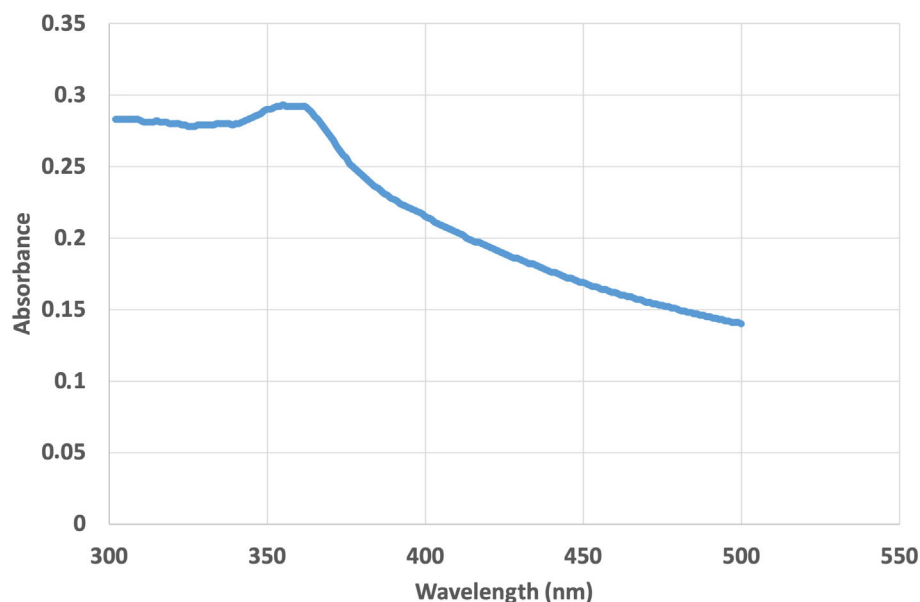


FIGURE 1 Synthesis of zinc oxide nanoparticles (NPs) using *Calendula officinalis* flower extract. (A) *C. officinalis* flower aqueous extract; (B) zinc nitrate hexahydrate solution; (C) colour of *C. officinalis* extract and zinc oxide hexahydrate mixture before heating; (D) pale yellow precipitate formation indicating the synthesis of ZnO NPs.

FIGURE 2 UV-Vis absorbance spectrum at 355 nm maximum of zinc oxide nanoparticles (NPs) synthesized using an aqueous extract from flowers of *Calendula officinalis* (Co-ZnO NPs).



355 nm was observed, which is specific for Co-ZnO NPs. In a similar study in which ZnO NPs were synthesized by green synthesis method using *Thymbra spicata* L. plant extract, they observed an absorbance peak at 360 nm when they examined the UV-Vis spectrum.⁴⁵ It was observed that the ZnO NPs synthesised by Pehlivanoglu et al.⁴⁶ with grape seed extract exhibited a strong absorbance peak at 362 nm, consistent with our study.

Green-synthesised Co-ZnO NPs were subjected to SEM and EDS analyses to determine surface morphology and elemental composition, respectively. The topographic image obtained via SEM showed aggregation of Co-ZnO NPs (Figure 3A), while the EDS spectrum confirmed that the elementary composition of the particles consisted largely of Zn and O elements. In particular, the elemental composition of Zn and O was 42.90% and 29.71%, respectively (Figure 3B). At the same time, the EDS spectrum of Co-ZnO NPs shows peaks of C, Na, Mg, Al and P

elements. These minimal elements were probably caused by residues of *C. officinalis*. A major zinc peak of 2.88 keV confirms the elemental distribution of Co-ZnO NPs. When the SEM image (Figure 3A) of Co-ZnO NPs is examined, nano-sized particles are seen, mostly spherical, some of which are irregular in shape. Similar results were also reported for green-synthesised ZnO NPs from various other medicinal plants.^{47,48}

Figure 4 illustrates the XRD patterns of green-synthesised Co-ZnO NPs. The characteristic diffraction peaks were revealed at 2θ values 31.85, 34.52, 36.35, 47.64, 56.71, 62.96, 66.46, 68.07, 69.22, 72.74 and 77.07 degrees and can be indexed to the diffractions of (100), (002), (101), (102), (110), (103), (200), (112), (201), (004) and (202) planes with a hexagonal wurtzite structure. All the peaks in the XRD graph of ZnO NPs are well matched with the COD database no. 96-901-1663. The XRD patterns of the green-synthesised ZnO NPs were very similar to the previous

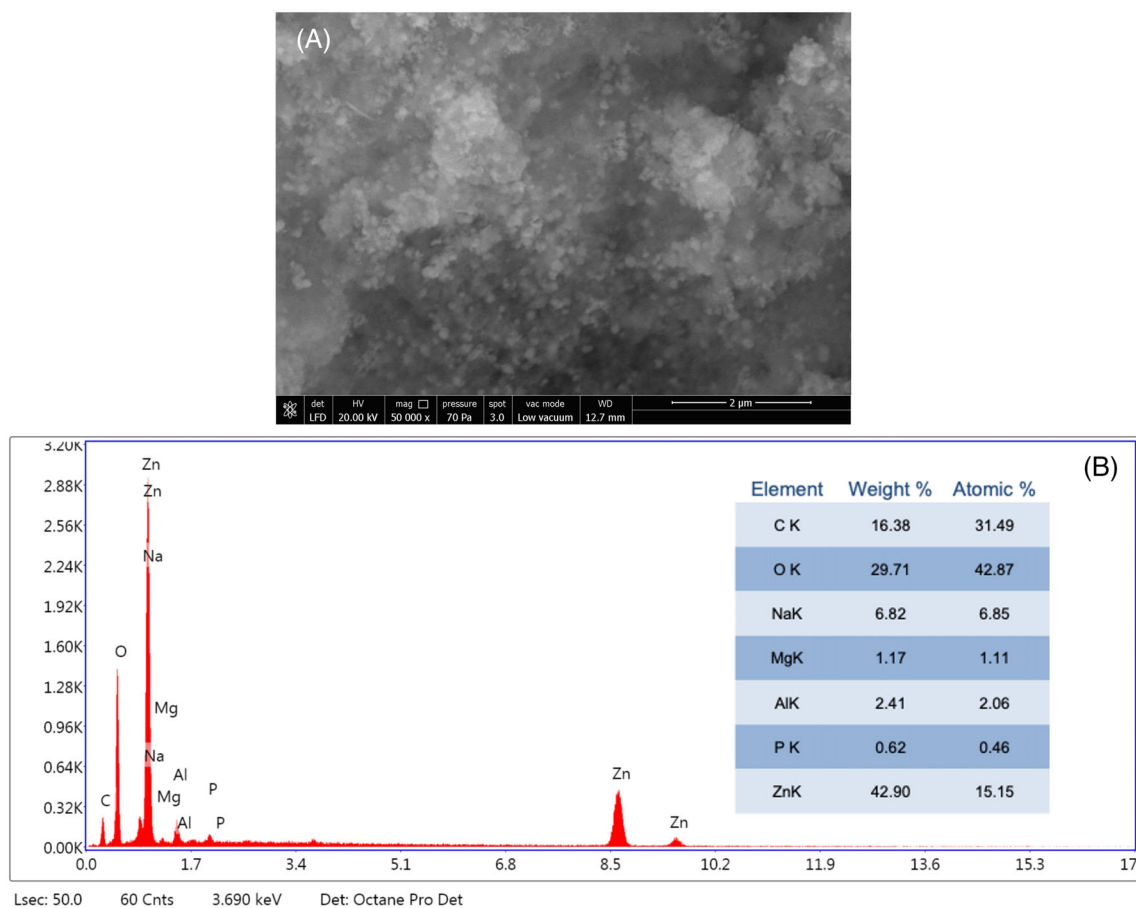


FIGURE 3 (A) Scanning electron microscope image and (B) Energy-dispersive X-ray spectroscopy analysis of synthesized Co-ZnO nanoparticles.

finding.⁴⁹ The average crystallite size of green-synthesized ZnO NPs was calculated using the Debye–Scherrer equation and found to be 17.66 nm (Table 1).

$$D = \frac{0.89 \lambda}{\beta \cos \theta}$$

where D is the crystallite size; k is the Scherrer constant; λ is the x-ray wavelength; θ is the Bragg angle and β is the full-width half maxima.

3.2 | Cytotoxic effects of Co-ZnO NPs

The effect of Co-ZnO NPs on cell viability was evaluated by the MTT assay at different concentrations (1, 5, 10, 20, 30, 40, 50, 100, 200 $\mu\text{g}/\text{mL}$) over a 48-h period in L929 fibroblast cell line. The growth of the exposed cells was compared with negative control cultured cells not treated with Co-ZnO NPs. The cytotoxicity of green-synthesized Co-ZnO NPs in L929 cells was found to be dose-dependent (Figure 5A). As the concentration increased, the cytotoxicity level also increased. At the

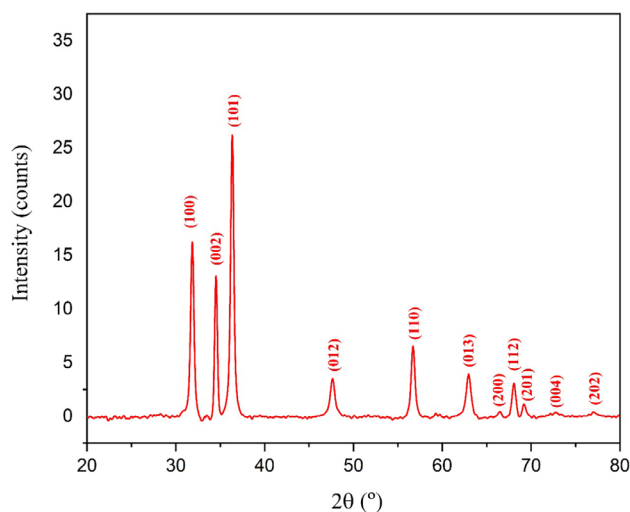


FIGURE 4 X-ray diffractometer pattern of synthesized Co-ZnO nanoparticles.

highest concentration tested (200 $\mu\text{g}/\text{mL}$), 95.8% of cell death was observed. The IC_{50} value was determined as 25.96 $\mu\text{g}/\text{mL}$ (Figure 5B). The results showed that 10 $\mu\text{g}/\text{mL}$ and lower concentrations could be used as non-toxic dose

TABLE 1 Crystalline size and miller indices (Hkl) value of observed crystalline peaks.

Peak position 2 θ (°)	Hkl	Crystalline size (nm)	Average crystalline size (nm)
31.85	100	21.29	17.66
34.52	002	25.48	
36.35	101	21.52	
47.64	012	15.21	
56.71	110	19.78	
62.96	013	15.05	
66.46	200	18.37	
68.07	112	16.57	
69.22	201	19.87	
72.74	004	7.32	
77.07	202	13.86	

to evaluate the in vitro wound healing activity of synthesized Co-ZnO NPs.

3.3 | Efficacy of Co-ZnO NPs on wound healing in vitro

The in vitro wound healing (scratch test) assay is a useful technique in which the migration and proliferation potentials of cells are evaluated under various conditions. In this method, a line that mimics the wound is created with a micropipette tip in cells that proliferate in a single layer, and the extent to which this wound is closed by applying therapeutic agents to the cells is measured and compared with the control group.⁵⁰ In the study, the therapeutic dose (10 $\mu\text{g/mL}$) determined by the MTT test was used to evaluate the therapeutic efficacy of Co-ZnO NPs on the wound model created by the scratch assay in

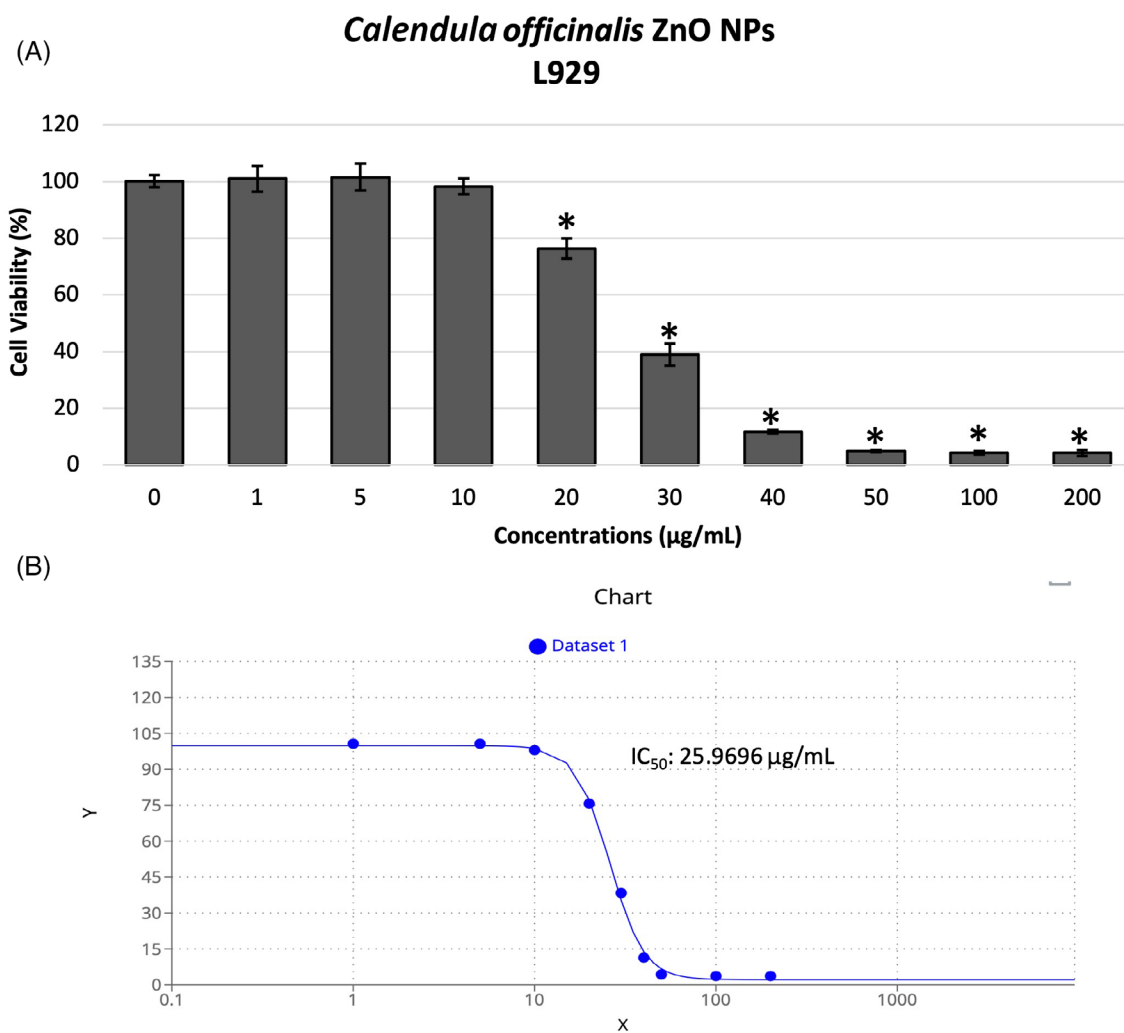


FIGURE 5 (A) Cell viability of L929 fibroblast cells after treatment (48 h) with various concentrations of green-synthesised Co-ZnO nanoparticles (NPs) in comparison with untreated cells (negative control) evaluated in MTT assay. (B) The IC_{50} value calculated in GraphPad Prism software on the basis of MTT assay. * $p < 0.05$.

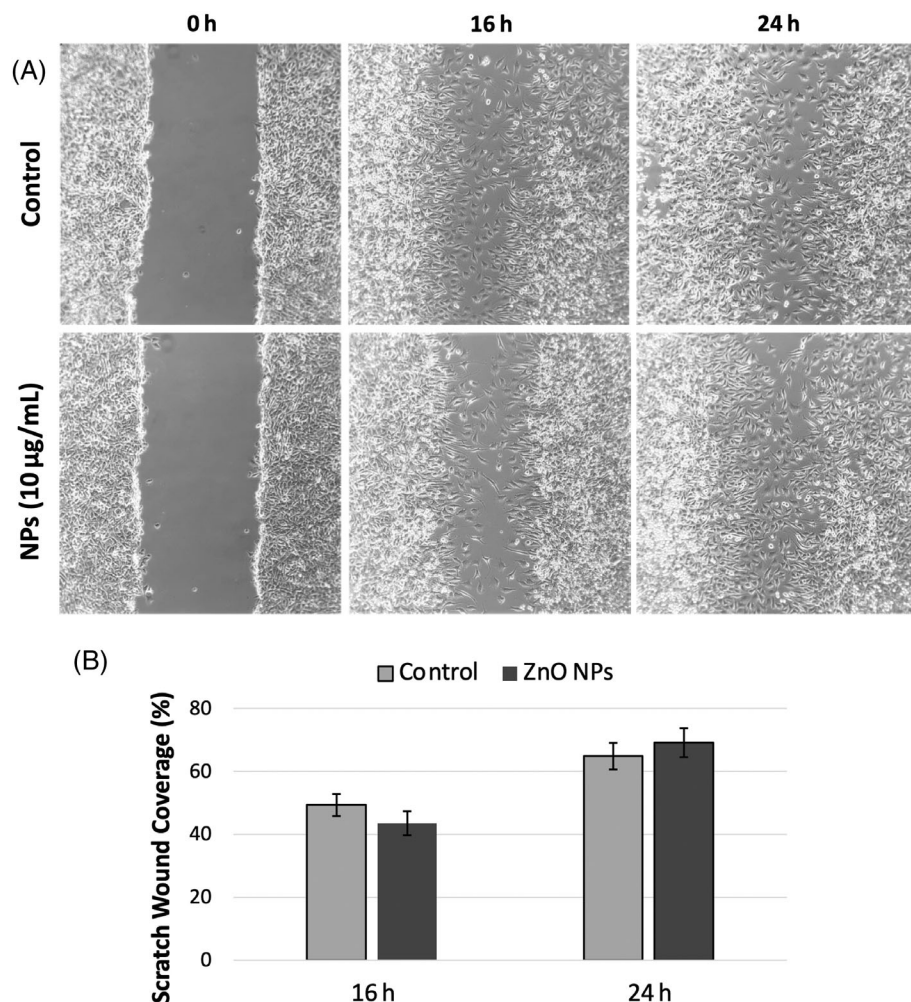


FIGURE 6 (A) In vitro wound healing assay images of L929 fibroblast cells obtained at 16 and 24 h after wound creation (Co-ZnO nanoparticles [NPs]-10 µg/mL). (B) Percentage wound closure graph of L929 fibroblast cells. Results are expressed as mean \pm SEM.

L929 cells (Figure 6A). After the treatment of Co-ZnO NPs synthesized by *C. officinalis* to L929 cells at a concentration of 10 µg/mL, an increase in wound closure of these cells was observed at 24 h compared with the control group (Figure 6B). The wound healing potential of Co-ZnO NPs was confirmed by the wound scratch test. *C. officinalis* ZnO NPs showed partial cell migration and percent wound closure (69.1%) compared with control (64.8%). This result demonstrated the wound healing potential of formulated Co-ZnO NPs. Erdoğan and Cevik⁵¹ synthesized ZnO NPs by microwave method using *Saccharomyces cerevisiae* aqueous lysate in their study to determine the in vitro wound healing efficiency of ZnO NPs. In their study, it was determined that L929 cells treated with ZnO NP did not have a dose-dependent toxic effect and the wound closure amount of L929 cells treated with 10, 100 and 1000 µg/mL ZnO NPs increased significantly compared with the control group cells. Kabeerdass et al.⁵² reported that ZnO NPs synthesized with the leaf extract of *Altermanthera sessilis* had better wound healing in L929 cells than in control. Vakayil et al.⁵³ investigated the wound healing potential of

Boswellia serrata-mediated synthesized ZnO NPs (BS-ZnO NPs) by in vitro wound scratch assay using L929 cells. The results of the scratch test revealed that BS-ZnO NPs increased L929 cell migration and increased wound closure rate. Both concentrations of BS-ZnO NPs (15 and 20 µg/mL) improved cell migration and thus rapidly closed the scar.

3.4 | Antioxidant activity of Co-ZnO NPs

The maximum concentration of Co-ZnO NPs (1000 µg/mL) significantly inhibited both DPPH and ABTS free radicals up to 33.49% and 46.63%, respectively (Figure 7A,B). Co-ZnO NPs have acceptable antioxidant activity. Dianati et al.⁵⁴ reported that curcumin-mediated Cm-ZnO NPs determined antioxidant activity with DPPH and ABTS at 500 µg/mL concentration as 18.06% and 21.033%, respectively. In our study, on the other hand, at 500 µg/mL Co-ZnO NP concentration, DPPH and ABTS and antioxidant activity were 32.37% and 32.25%, respectively. Ihsan et al.⁵⁵ reported ABTS activities (46.05% and

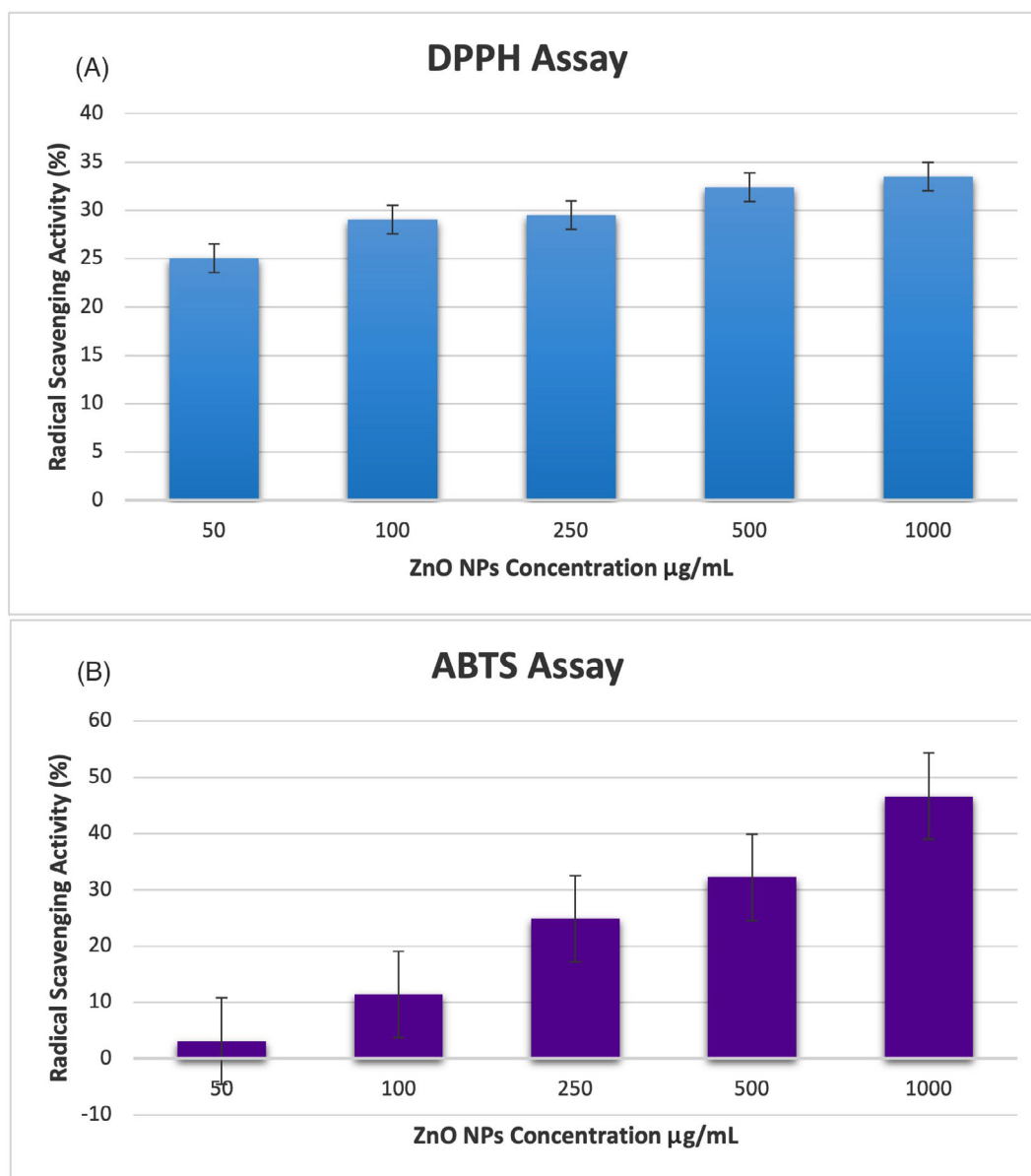


FIGURE 7 Antioxidant activity of Co-ZnO nanoparticles (NPs): (A) 2,2-Diphenyl-1-picrylhydrazyl radical (DPPH) and (B) 2,2'-azino-bis(3-ethylbenzothiazoline-6-sulfonic acid) (ABTS) radical scavenging activities.

42.79%) and DPPH activities (58.16% and 55.76%) in 1000 µg/mL of *Curcuma zedoaria* and *Momordica charantia*-mediated synthesized ZnO NPs, respectively. The fact that ZnO NPs prepared from various plant extracts have different sizes and consequently different specific surfaces depending on the plant extract used may be the reason for the differences in the antioxidant activity of ZnO NPs.

4 | CONCLUSION

Metallic NPs are an area of interest due to their unique properties that may be advantageous for producing

targetable products. ZnO NPs have been used frequently in the pharmaceutical industry in recent years due to their strong biological activities. In this study, it was tried to develop antioxidant ZnO NPs with wound healing activity from *C. officinalis* flowers using an environmentally friendly green synthesis method. Synthesized Co-ZnO NPs were characterized by UV-Vis spectroscopy, SEM-EDS and XRD techniques. Biosynthesized Co-ZnO NPs did not show cytotoxic effects at low concentrations but exhibited better wound healing effects compared with control. It also showed substantial antioxidant activity. Therefore, the synthesis of drugs based on medicinal or combined Co-ZnO NPs with greater targeted activity, synthesized from *C. officinalis* flowers, may lead to

opportunities for the discovery of a cheaper and more beneficial therapy for wound healing. However, the wound healing effects of Co-ZnO NPs need to be supported by in vivo findings.

ACKNOWLEDGEMENTS

This research was supported by the Burdur Mehmet Akif Ersoy University Scientific Research Projects Unit (Project number: 0792-YL-21). The authors are thankful to Suleyman Demirel University YETEM—Innovative Applications and Research Center.

CONFLICT OF INTEREST STATEMENT

The authors declare no conflict of interest.

DATA AVAILABILITY STATEMENT

Data available on request from the authors.

ORCID

Cigdem Aydin Acar  <https://orcid.org/0000-0002-1311-2314>

Muhammet Abdurrahim Gencer  <https://orcid.org/0009-0004-6876-8646>

Suray Pehlivanoglu  <https://orcid.org/0000-0001-7422-2974>

Sukriye Yesilot  <https://orcid.org/0000-0003-3354-8489>

Soner Donmez  <https://orcid.org/0000-0003-0328-6481>

REFERENCES

- World Health Organization. Programme on Traditional Medicine. *WHO Traditional Medicine Strategy 2002–2005*. World Health Organization; 2002. <https://apps.who.int/iris/handle/10665/67163>
- Jackson RA, Hawa MI, Jaspan JB, et al. Mechanism of metformin action in non-insulin-dependent diabetes. *Diabetes*. 1987; 36(5):632-640.
- Dobs AS, Goldstein BJ, Aschner P, et al. Efficacy and safety of sitagliptin added to ongoing metformin and rosiglitazone combination therapy in a randomized placebo-controlled 54-week trial in patients with type 2 diabetes. *J Diabetes*. 2013;5:68-79.
- Patel D, Prasad S, Kumar R, Hemalatha S. An overview on antidiabetic medicinal plants having insulin mimetic property. *Asian Pac J Trop Biomed*. 2012;2:320-330.
- Nabeel MA, Kathiresan K, Manivannan S. Antidiabetic activity of the mangrove species *Ceriops decandrain* alloxan-induced diabetic rats. *J Diabetes*. 2010;2:97-103.
- Powell SR. The antioxidant properties of zinc. *J Nutr*. 2000; 130(5S suppl):1447S-1454S.
- Adachi Y, Yoshida J, Koderu Y, et al. Oral administration of a zinc complex improves type 2 diabetes and metabolic syndromes. *Biochem Biophys Res Commun*. 2006;351(1):165-170.
- Pino P, Bosco F, Mollea C, Onida B. Antimicrobial nano-zinc oxide biocomposites for wound healing applications: a review. *Pharmaceutics*. 2023;15(3):970.
- Bandeira M, Chee BS, Frassini R, et al. Antimicrobial PAA/PAH electrospun fiber containing green synthesized zinc oxide nanoparticles for wound healing. *Materials (Basel)*. 2021; 14(11):2889.
- Gilaki M. Biosynthesis of silver nanoparticles using plant extracts. *Aust J Biol Sci*. 2010;10(5):465-467.
- Raveendran P, Fu J, Scott L. Completely green synthesis and stabilization of metal nanoparticles. *J Am Chem Soc*. 2003;125: 13940-13941.
- Erdoğan Ö, Birtekocak F, Oryaşın E, et al. Green synthesis, characterization, anti-bacterial and cytotoxic effects of zinc oxide nanoparticles using aqueous extract of artichoke leaves. *Duzce Med J*. 2019;21(1):19-26.
- Sahu AN. Nanotechnology in herbal medicines and cosmetics. *Int Res Ayurveda Pharma*. 2013;4(3):472-474.
- Parveen K, Banse V, Ledwani L. Green synthesis of nanoparticles: their advantages and disadvantages. *AIP Conf Proc*. 2016; 1724(1):020048.
- Agarwal H, Venkat Kumar S, Rajeshkumar S. A review on green synthesis of zinc oxide nanoparticles – an eco-friendly approach. *Resour Effic Technol*. 2017;3(4):406-413.
- Abdul Salam H, Sivaraj R, Venckatesh R. Green synthesis and characterization of zinc oxide nanoparticles from *Ocimum basilicum* L. var. *purpurascens* Benth.-Lamiaceae leaf extract. *Mater Lett*. 2014;131:16-18.
- Rajendran SP, Sengodan K. Synthesis and characterization of zinc oxide and iron oxide nanoparticles using *Sesbania grandiflora* leaf extract as reducing agent. *J Nanosci*. 2017;2017:8348507.
- Yuvakkumar R, Suresh J, Nathanael AJ, Sundrarajan M, Hong SI. Novel green synthetic strategy to prepare ZnO nanocrystals using rambutan (*Nephelium lappaceum* L.) peel extract and its antibacterial applications. *Mater Sci Eng C Mater Biol Appl*. 2014;41:17-27.
- Ramesh P, Rajendran A, Meenakshisundaram M. Green synthesis of zinc oxide nanoparticles using flower extract *Cassia Auriculata*. *J Nanosci Nanotechnol*. 2014;1(1):41-45.
- Rouhi J, Mahmud S, Naderi N, Ooi CR, Mahmood MR. Physical properties of fish gelatin-based bio-nanocomposite films incorporated with ZnO nanorods. *Nanoscale Res Lett*. 2013;8:364.
- Mittal AK, Chisti Y, Banerjee UC. Synthesis of metallic nanoparticles using plant extracts. *Biotechnol Adv*. 2013;31:346-356.
- Kairyte K, Kadys A, Luksiene Z. Antibacterial and antifungal activity of photoactivated ZnO nanoparticles in suspension. *J Photochem Photobiol B*. 2013;128:78-84.
- Kajbafvala A, Ghorbani H, Paravar A, Samberg JP, Kajbafvala E, Sadrnezhad SK. Effects of morphology on photocatalytic performance of zinc oxide nanostructures synthesized by rapid microwave irradiation methods. *Superlattices Microstruct*. 2012;51(4):512-522.
- Kumar SS, Venkateswarlu P, Rao VR, Rao GN. Synthesis, characterization and optical properties of zinc oxide nanoparticles. *Int Nano Lett*. 2013;3:30.
- Sundrarajan M, Ambika S, Bharathi K. Plant extract mediated synthesis of ZnO nanoparticles using *Pongamia pinnata* and their activity against bacteria. *Adv Powder Technol*. 2015;26:1294-1299.
- Elumalai K, Velmurugan S, Ravi S, Kathiravan V, Adaikala RG. Bio-approach: plant mediated synthesis of ZnO nanoparticles and their catalytic reduction of methylene blue and antimicrobial activity. *Adv Powder Technol*. 2015;26:1639-1651.
- Shekhawat MS, Ravindran CP, Manokari M. A green approach to synthesize the zinc oxide nanoparticles using aqueous extracts of *Ficus benghalensis* L. *Int J Biosci Agric Technol*. 2015;6:1-5.
- Mishra V, Sharma R. Green synthesis of zinc oxide nanoparticles using fresh peels extract of *Punica granatum* and its antimicrobial activities. *Int J Pharm Res Health Sci*. 2015;3:694-699.

29. Dobrucka R, Długaszewska J. Biosynthesis and antibacterial activity of ZnO nanoparticles using *Trifolium pratense* flower extract. *Saudi J Biol Sci*. 2016;23:517-523.
30. Bala N, Saha S, Chakraborty M, et al. Green synthesis of zinc oxide nanoparticles using *Hibiscus subdariffa* leaf extract: effect of temperature on synthesis, antibacterial activity and anti-diabetic activity. *RSC Adv*. 2015;5:4993-5003.
31. Manokari M, Shekhawat MS. Biogenesis of zinc oxide nanoparticles using *Couroupita guianensis* Aubl. extracts – a green approach. *World Sci News*. 2016;29:135-145.
32. Parente LM, Lino Júnior Rde S, Tresvenzol LM, Vinaud MC, de Paula JR, Paulo NM. Wound healing and anti-inflammatory effect in animal models of *Calendula officinalis* L. growing in Brazil. *Evid Based Complement Alternat Med*. 2012;2012:375671.
33. Brown DJ, Dattner AM. Phytotherapeutic approaches to common dermatologic conditions. *Arch Dermatol*. 1998;134(11):1401-1404.
34. Re TA, Mooney D, Antignac E, et al. Application of the threshold of toxicological concern approach for the safety evaluation of calendula flower (*C. officinalis*) petals and extracts used in cosmetic and personal care products. *Food Chem Toxicol*. 2009;47(6):1246-1254.
35. Kavya JB, Murali M, Manjula S, et al. Genotoxic and antibacterial nature of biofabricated zinc oxide nanoparticles from *Sida rhombifolia* Linn. *J Drug Deliv Sci Technol*. 2020;60:101982.
36. Aydin Acar C, Pehlivanoglu S. Biosynthesis of silver nanoparticles using *Rosa canina* extract and its anti-cancer and anti-metastatic activity on human colon adenocarcinoma cell line HT29. *MAKU J Health Sci Inst*. 2019;7(2):124-131.
37. Aydin Acar C, Pehlivanoglu S, Yesilot S, Yakut US. Microwave-assisted biofabrication of silver nanoparticles using *Helichrysum arenarium* flower extract: characterization and biomedical applications. *Biomass Convers Biorefin*. 2023. doi:10.1007/s13399-023-03833-6
38. Re R, Pellegrini N, Proteggente A, Pannala A, Yang M, Rice- EC. Antioxidant activity applying an improved ABTS radical cation decolorization assay. *Free Radic Biol Med*. 1999;26(9-10):1231-1237.
39. Donmez S, Keyvan E. Green synthesis of zinc oxide nanoparticles using grape seed extract and evaluation of their antibacterial and antioxidant activities. *Inorg Nano-Met Chem*. 2023. doi:10.1080/24701556.2023.2165687
40. Singh J, Dutta T, Kim KH, Rawat M, Samddar P, Kumar P. 'Green' synthesis of metals and their oxide nanoparticles: applications for environmental remediation. *J Nanobiotechnol*. 2018;16(1):84.
41. Naseer M, Aslam U, Khalid B, Chen B. Green route to synthesize zinc oxide nanoparticles using leaf extracts of *Cassia fistula* and *Melia azadarach* and their antibacterial potential. *Sci Rep*. 2020;10(1):9055.
42. Rajiv P, Rajeshwari S, Venkatesh R. Bio-fabrication of zinc oxide nanoparticles using leaf extract of *Parthenium hysterophorus* L. and its size-dependent antifungal activity against plant fungal pathogens. *Spectrochim Acta A Mol Biomol Spectrosc*. 2013;112:384-387.
43. Balciunaitiene A, Puzeryte V, Radenkova V, et al. Sustainable-green synthesis of silver nanoparticles using aqueous *Hyssopus officinalis* and *Calendula officinalis* extracts and their antioxidant and antibacterial activities. *Molecules*. 2022;27(22):7700.
44. Hernández-Díaz JA, Garza-García JJ, León-Morales JM, et al. Antibacterial activity of biosynthesized selenium nanoparticles using extracts of *Calendula officinalis* against potentially clinical bacterial strains. *Molecules*. 2021;26(19):5929.
45. Gur T, Meydan I, Seckin H, Bekmezci M, Sen F. Green synthesis, characterization and bioactivity of biogenic zinc oxide nanoparticles. *Environ Res*. 2022;204(Pt A):111897.
46. Pehlivanoglu S, Aydin Acar C, Donmez S. Characterization of green synthesized flaxseed zinc oxide nanoparticles and their cytotoxic, apoptotic and antimigratory activities on aggressive human cancer cells. *Inorg Nano-Met Chem*. 2021. doi:10.1080/24701556.2021.1980034
47. Rana N, Chand S, Gathania AK. Green synthesis of zinc oxide nano-sized spherical particles using *Terminalia chebula* fruits extract for their photocatalytic applications. *Int Nano Lett*. 2016;6:91-98.
48. El-Hawwary SS, Abd Almaksoud HM, Saber FR, et al. Green-synthesized zinc oxide nanoparticles, anti-Alzheimer potential and the metabolic profiling of *Sabal blackburniana* grown in Egypt supported by molecular modelling. *RSC Adv*. 2021;11(29):18009-18025.
49. Cárdenas KA, Domínguez J, Palacios E, García L, Ramírez PA, Flores M. Synthesis and characterization of ZnO nanoparticles obtained from the extract of *Schinus molle*. In: Li J, Zhang M, Li B, Monteiro SN, Ikhmayies S, Kalay YE, Hwang JY, Escobedo-Díaz JP, Carpenter JS, Brown AD, Soman R, Moser A, eds. *The Minerals, Metals and Materials Series 2021*. Springer International Publishing; 2021:569-575.
50. Keese CR, Wegener J, Walker SR, Giaeffer I. Electrical wound-healing assay for cells in vitro. *Proc Natl Acad Sci U S A*. 2004;101(6):1554-1559.
51. Erdoğan Ö, Cevik O. Investigation of the effects of zinc oxide nanoparticles synthesized by *Saccharomyces cerevisiae* aqueous lysate on in-vitro wound healing model. *J Adnan Menderes Uni HealthSci Fac*. 2023;7(1):127-135.
52. Kabeerdass N, Thangasamy S, Murugesan K, et al. Embedding green synthesized zinc oxide nanoparticles in cotton fabrics and assessment of their antibacterial wound healing and cytotoxic properties: an eco-friendly approach. *Green Process Synth*. 2022;11(1):875-885.
53. Vakayil R, Ramasamy S, Alahmadi TA, Almoallim HS, Natarajan N, Mathanmohun M. *Boswellia serrata*-mediated zinc oxide nanoparticles-coated cotton fabrics for the wound healing and antibacterial applications against nosocomial pathogens. *Appl Nanosci*. 2022;12:2873-2887.
54. Dianati E, Hojati V, Khayatzadeh J, Zafar BS. The green-synthesized curcumin-mediated zinc oxide nanoparticles (CmZnO-NP) as the exclusive antioxidant and efficient wound healing agent compared with curcumin, methanol, phenytoin, and ZnO. *Inorg Nano-Met Chem*. 2021. doi:10.1080/24701556.2021.1956964
55. Ihsan M, Din IU, Alam K, Munir I, Mohamed HI, Khan F. Green fabrication, characterization of zinc oxide nanoparticles using plant extract of *Momordica charantia* and *Curcuma zedoaria* and their antibacterial and antioxidant activities. *Appl Biochem Biotechnol*. 2023;195:1-20.

How to cite this article: Aydin Acar C, Gencer MA, Pehlivanoglu S, Yesilot S, Donmez S. Green and eco-friendly biosynthesis of zinc oxide nanoparticles using *Calendula officinalis* flower extract: Wound healing potential and antioxidant activity. *Int Wound J*. 2024;21(1):e14413. doi:10.1111/iwj.14413